AP2-dependent signals from the ectoderm regulate craniofacial development in the zebrafish embryo

Robert D. Knight, Yashar Javidan, Tailin Zhang, Sarah Nelson and Thomas F. Schilling*

Department of Developmental and Cell Biology, University of California, Irvine, CA 92697-2300, USA
*Author for correspondence (e-mail: tschilli@uci.edu)

Accepted 26 April 2005

Development 132, 3127-3138
Published by The Company of Biologists 2005
doi:10.1242/dev.01879

Summary

AP2 transcription factors regulate many aspects of embryonic development. Studies of AP2a (Tfap2a) function in mice and zebrafish have demonstrated a role in patterning mesenchymal cells of neural crest origin that form the craniofacial skeleton, while the mammalian Tfap2b is required in both the facial skeleton and kidney. Here, we show essential functions for zebrafish *tfap2a* and *tfap2b* in development of the facial ectoderm, and for signals from this epithelium that induce skeletogenesis in neural crest cells (NCCs). Zebrafish embryos deficient for both *tfap2a* and *tfap2b* show defects in epidermal cell survival and lack NCC-derived cartilages. We show that cartilage defects arise after NCC migration during skeletal differentiation, and that they can be rescued by transplantation of wild-type ectoderm. We propose a model in which AP2 proteins play two distinct roles in cranial NCCs: an early cell-autonomous function in cell specification and survival, and a later non-autonomous function regulating ectodermal signals that induce skeletogenesis

Key words: Tcfap2, Neural crest, Craniofacial, *Danio rerio*

Introduction

Vertebrate neural crest cells (NCCs) form all body pigmentation, peripheral neurons and glia, and most skull cartilage and bone. Some skeletogenic NCCs surround the brain to form the skull vault, while others migrate into the pharyngeal arches to form the jaw and larynx, and defects in these cells underlie many craniofacial birth defects. Cranial NCCs carry positional information from their origins alongside the midbrain and hindbrain, but also receive inductive signals from surrounding epithelia that determine skeletal fates (Graham, 2003; Santagati and Rijli, 2003; Trainor et al., 2003). Molecular mechanisms underlying these epithelial-mesenchymal interactions between NCCs and facial endoderm or ectoderm are largely unknown.

AP2 transcription factors are highly conserved DNA-binding proteins implicated in cranial NCC development. Three of the five members of this family in mammals (*Tcfap2a*, *Tcfap2b* and *Tcfap2g*) are expressed in migrating NCCs (Moser et al., 1995; Hilger-Eversheim et al., 2000). *Tcfap2a*$^{-/-}$ mutant mice have defects in the neural tube, body wall and limbs, and striking malformations of NCC-derived craniofacial structures (palate and ear ossicles) that correlate with defects in NCC survival (Schorle et al., 1996; Zhang et al., 1996; Morris-Kay et al., 1996). Craniofacial defects, however, could be indirectly due to disruptions in neural tube and epithelial morphogenesis in *Tcfap2a*$^{-/-}$ mutants, because early NCC migration appears grossly unaffected (Schorle et al., 1996). *Tcfap2b*$^{-/-}$ mutant mice and *TFAP2B*$^{+/-}$ humans have renal epithelial apoptosis and patent ductus arteriosus (Char syndrome), and mild defects in the NCC-derived craniofacial skeleton (Chazaud et al., 1996; Moser et al., 1997b; Satoda et al., 2000). The only defects reported in *Tcfap2g*$^{-/-}$ mutant mice are placental (Auman et al., 2002). Thus, co-expression and conserved protein structures of *Tcfap2a* and *Tcfap2b* suggest that their functions are redundant, but specific requirements in NCCs remain unclear.

Insights into *tfap2a* function in NCCs have come from analysis of the zebrafish *lockjaw* (*low*^{ts213}) mutation, which eliminates *tfap2a* function but lacks the severe neural tube defects seen in *Tcfap2a*$^{-/-}$ mice. *low*^{ts213} mutants have early defects in NCC specification, prior to migration, and later lack subsets of cartilage and pigment cells (Schilling et al., 1996; Knight et al., 2003). *low/tfap2a* is required for *kit* expression in pigment cell precursors and differentiation of early melanocytes and iridophores (Knight et al., 2004), and previous studies of the mammalian *KIT* promoter suggests that this regulation is direct (Huang et al., 1998). Similar to studies of the *Hoxa2* promoter in mice (Maconochie et al., 1999), zebrafish *low/tfap2a* is required to activate transcription of Hox group 2 genes in NCCs of the second pharyngeal arch (hyoid), suggesting that *tfap2a* regulates the segmental identities of NCCs (Knight et al., 2004). Hyoid defects and fusions with the mandibular arch in *low* mutants also resemble embryos lacking *hoxa2/hoxb2* gene functions (Hunter and Prince, 2002). These studies demonstrate a cell-autonomous role for *tfap2a* in subsets of NCC, but cannot account for more widespread defects in NCC survival and chondrogenesis in AP2-deficient embryos (Schorle et al., 1996; Knight et al., 2003; Barrallo-Gimeno et al., 2004). Thus, *Tcfap2a* may have additional, non-autonomous roles in the tissues with which NCCs interact.

Tcfap2a was previously known as keratin transcription factor, *KTF-1*, a regulator of epidermal differentiation in vitro

(Leask et al., 2001). *Tcfap2a*$^{-/-}$ mutant mice and zebrafish have normal skin architecture, suggesting that other AP2 family members can compensate in vivo. However, this has not been carefully examined in facial ectoderm, where specialized domains of pharyngeal ectoderm interact with NCCs in a similar way to the apical ectoderm of the limb bud, and these may depend on AP2 (Wall and Hogan, 1995; Hu and Helms, 1999). The pharyngeal ectoderm induces cartilage in mammals (Hall, 1980) and expresses signaling molecules (e.g. Fgf8, Shh, Bmp4) involved in craniofacial development. Fgf8 from the oral ectoderm patterns the mouse mandible (Trumpp et al., 1999; Tucker et al., 1999; Abu-Issa et al., 2002; Macatee et al., 2003), while Fgf4, Fgf9, Fgf17 and Fgf18 from pharyngeal ectoderm pattern other bones and teeth (Kettunen and Thesleff, 1998; Bachler and Neubuser, 2001). Shh signaling is required for patterning many regions of the skull, including the jaw and facial midline, and recent evidence suggest that this is a direct effect on NCCs (Jeong et al., 2004). Thus, multiple ectodermal signals converge on NCCs to control growth and patterning. NCCs also signal back to the overlying ectoderm to maintain ectodermal development (Creuzet et al., 2004).

In this study, we identify *tfap2b* as a pivotal factor in craniofacial skeletal development in zebrafish. *tfap2b* is expressed in the pharyngeal ectoderm, not in NCCs, and the combined loss of *tfap2b* and *tfap2a* function leads to defects in NCC-derived pharyngeal cartilages. Grafts of pharyngeal ectoderm into AP2-deficient embryos restores cartilage development. Taken together, these findings indicate that *tfap2b* and its close relative, *tfap2a*, play redundant roles in the ectoderm to control skeletogenesis of NCCs. This is the first in vivo demonstration of a requirement for AP2 transcription factors in the ectoderm, and strong evidence for redundant functions among AP2 family members.

Materials and methods

Animals and histology

Zebrafish embryos were obtained in natural crosses and staged according to Kimmel et al. (Kimmel et al., 1995). The *low*^{ts213} allele of *tfap2a* was originally isolated in the 1996 ENU mutagenesis screen in Tübingen (Schilling et al., 1996) and for this study was crossed into AB and *fli1-GFP* transgenic backgrounds (Lawson and Weinstein, 2002). *low* mutants were identified by their lack of early melanocytes at 25 hpf (Schilling et al., 1996; Knight et al., 2003). Cartilages were visualized by Alcian Blue staining and flat mounted (Kimmel et al., 1998; Javidan and Schilling, 2004).

Cloning and PCR amplification of *tfap2b* transcripts

Forward and reverse primers ap2b-7f (CGAGGCGAACGGACGG-AGCG) and ap2b-1r (CCTTCACCACATAACACC) were designed to EST sequences fp02d11.y1 (GenBank Accession Number BG737469) and fp60d09.x1 (GenBank Accession Number BI671067), respectively. A 3.1 kb band corresponding to the full-length *tfap2b* (GenBank Accession Number DQ060246) was amplified by RT-PCR from 26 hpf embryos. This was cloned into pGEM T'Easy (Promega), completely sequenced in both directions using the Big Dye Terminator Sequencing reagent (ABI), and run on an ABI PRISM 310 sequencer (PE Applied Biosystems). RT-PCR amplification of *tfap2b* over exon 5 in morpholino-injected animals and for staging of *tfap2b* expression used 10 pmol each of primers ap2b-6f (AGAGCGGAGGTTTACTG) and ap2b-6r (ATGTGACATT-CGCTGCC) with a slightly lower annealing temperature of 50°C for 30 seconds.

Whole-mount in situ hybridization and immunohistochemistry

In situ hybridization was carried out as described previously (Thisse et al., 1993). Antisense probe for *tfap2b* was synthesized with SP6 RNA polymerase from the amplified *tfap2b* clone following linearization by *Nco*I. Probes and antibodies used were *dlx2* (Akimenko et al., 1994), *hoxa2* (Prince at al., 1998), *tfap2a* and *fgf8* (Furthauer et al., 1997), *fli1* (Brown et al., 2000), *gsc* (Stachel et al., 1993), *nkx2.3* (Lee et al., 1996), *sef* (Furthauer et al., 2002; Tsang et al., 2002), and *sox9b* (Li et al., 2002). Sectioning was performed after in situ hybridization. Embryos were immersed in 30% sucrose, embedded in 1% agar blocks, frozen in liquid nitrogen and cryostat sections cut at a thickness of 12 μm on a Leica cryostat.

Cell death detection assays

Apoptotic cell death was detected using a terminal transferase, dUTP nick-end labeling method (TUNEL) using several modifications suggested by the manufacturer (POD In Situ Cell Death Detection Kit, Roche). To avoid overfixing, embryos were dechorionated, and fixed in 4% PFA at 4°C overnight. They were then permeabilized with acetone at –20°C for 7 minutes and incubated in 2% goat serum at room temperature for 3 hours as a protein block prior to the TUNEL reaction. Apoptotic cells were counted in the pharyngeal region, between the posterior margin of the eye and anterior otic vesicle.

Morpholino injections

A morpholino ap2b-x5.1 (GCCATTTTTCGACTTCGCTCTGATC) was designed against the splice acceptor site of exon 5 in the *tfap2b* sequence at 1031 bp (Fig. 1B) by comparison with the corresponding genomic contig BX005121.8 from the zebrafish genome assembly (www.ensembl.org/D_rerio). The ap2b-x5.1 morpholino was reconstituted in 0.2M KCl and 3-5 ng was injected into one- or two-cell stage embryos together with 3% TRITC-dextran to act as a lineage tracer.

Ectoderm cell transplantation

Wild-type donor animals were injected with a combination of 3% TRITC-dextran (neutral, 10,000 M_r) and 3% biotin-dextran (lysine-fixable, 10,000 M_r) at the one- to two-cell stage. Cells within a few cell diameters of the animal pole were transplanted at the late blastula stage, as cell-tracing studies have shown that this region forms cranial ectoderm (Kimmel et al., 1990). Transplants in this position never formed endoderm or mesoderm, and were generally segregated in either non-neural ectoderm or in the neural tube and NCCs. Cells were transplanted into this location in *low* mutants and in wild-type siblings, and allowed to develop to 25 hpf, when transplanted cells were visualized by rhodamine fluorescence. Each embryo was then either: (1) fixed in 4% PFA and processed individually by in situ hybridization for *sef* expression, and detection of the biotin-labeled donor cells with a peroxidase coupled avidin-streptavidin complex (Vectastain) using DAB as the colored substrate; or (2) raised to 4 days postfertilization and processed for biotin detection and Alcian Blue staining for cartilage, as above.

Results

Cloning and characterization of zebrafish *tfap2b*

We previously showed a requirement for *tfap2a* in NCC development (Knight et al., 2003; Knight et al., 2004), and here we have analyzed the expression and function of a zebrafish *tfap2b*. Two ESTs were identified by sequence comparison with mammalian *Tcfap2b*. A 3.1 kb fragment amplified from cDNA of 26 hpf embryos showed high similarity at the amino acid level to *Tfap2b* genes from chick, mouse and human (E<0) compared with *Tfap2a* genes from

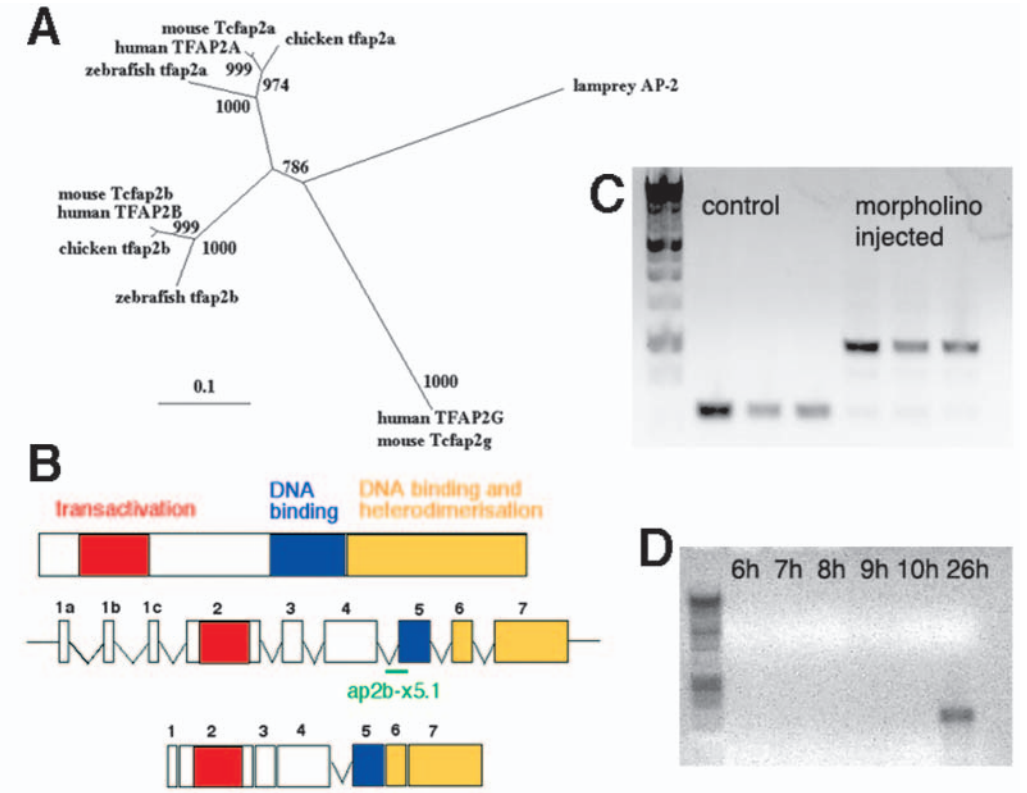

Fig. 1. Cloning and characterization of a zebrafish *tfap2b*. (A) Phylogenetic tree of AP2 genes shows zebrafish *tfap2b* more closely related to other vertebrate AP2b genes than to other zebrafish AP2 genes. Putative protein sequences of AP2 genes were aligned using ClustalX, edited by eye and used to generate a maximum likelihood tree by quartet puzzling using the PUZZLE program. Values at the nodes are likelihood values, showing support for that node out of 1000; branch lengths represent sequence divergence. (B) *tfap2b* contains the highly conserved transactivation (red), DNA-binding (blue) and heterodimerization domains (yellow) found in all AP2 proteins. Exon-intron boundaries are identical in *tfap2a* and *tfap2b*, and both have three alternative first exons (1a-c). A morpholino oligonucleotide directed against the splice acceptor site before exon 5 (ap2b-x5.1–'ap2bMO') should create a larger, unspliced product. (C) Splicing defects in *tfap2b* transcripts following ap2bMO injection. *tfap2b* was amplified from pools of ap2bMO-injected and control uninjected animals at 24 hpf using primers tfap2bf and tfap2br directed to exons 4 and 6, respectively. Uninjected animals showed PCR products of ~210 bp in size in comparison with ap2bMO-injected animals in which one larger product (~424 bp) was observed because of aberrant splicing. (D) PCR amplification of *tfap2b* from RNA isolated from different stages of zebrafish gastrulation fails to detect expression before 10 hpf.

zebrafish (E<–141), mouse (E<–143) and human (E<–146), and was designated *tfap2b*. Alignment with other family members revealed that *tfap2b* shares the highly conserved DNA binding and heterodimerization domains characteristic of all AP2 proteins (data not shown). Zebrafish *tfap2b* genes are more similar in sequence to *tfap2a* (65%) than to *tfap2g* (60%), *tfap2d* (52%) or *tfap2e* (63%), and vertebrate *Tfap2a* and *Tfap2b* group together while *Tfap2g* is more distantly related (Fig. 1A).

Using the whole zebrafish genome assembly (www.ensembl.org/Danio_rerio), we found that *tfap2b* has the same exon-intron arrangement as *tfap2a*, including exon-intron boundaries within the essential DNA-binding domain (Fig. 1B). To test *tfap2b* function during development, we designed an antisense morpholino (ap2bMO) to the splice acceptor site of *tfap2b* exon5 at 1030 bp in the mRNA sequence, an approach that we previously used successfully to disrupt *tfap2a* function (Knight et al, 2003). We used RT-PCR to show that injection of 5 ng ap2bMO per embryo disrupts splicing of *tfap2b* exon5 (Fig. 1C). We then sequenced the larger PCR product from ap2bMO-injected animals at 24 hpf and found that splicing failed at the intron-exon5 boundary, causing the intron to remain in the mRNA transcript. Similar splicing defects caused by a morpholino to *tfap2a* (ap2aMO) phenocopy the *lockjaw* mutant phenotype (Knight et al., 2003). The highly conserved exon-intron structures of AP2 genes, coupled with their nearly identical DNA binding and heterodimerization domains, suggests that the disruption of *tfap2b* splicing in ap2bMO-injected animals reflects a similar abrogation of *tfap2b* gene function as for *tfap2a*.

tfap2a and *tfap2b* are co-expressed in neural tube and ectoderm, but not neural crest

Unlike *tfap2a*, which is first expressed in the non-neural ectoderm during gastrulation and later in NCCs (Fig. 2A), *tfap2b* expression is first detected at six- to seven-somite stages in the hindbrain (Fig. 2B). Later, *tfap2a* is expressed throughout the surface ectoderm and in migrating NCCs, while *tfap2b* expression remains restricted to the hindbrain (Fig. 2C,D). Both genes are co-expressed in the developing intermediate mesoderm and by 24 hours postfertilization (hpf) in the pronephric ducts. *tfap2b* expression was not detected during gastrulation or early somitogenesis by in situ hybridization, or by RT-PCR on cDNA prepared from embryos harvested hourly between 6 and 10 hpf (Fig. 1D).

Surprisingly, *tfap2b* is not expressed in NCCs at any stage. Migrating NCCs in the pharyngeal arches express *tfap2a* at 24 hpf (Fig. 2E,G). At this stage, *tfap2b* is weakly expressed in the arches, but not in NCCs (Fig. 2F,H), and expression is restricted to surface pharyngeal ectoderm (see Fig. 6). By contrast, *tfap2a* is expressed in both NCCs and more broadly throughout the surface ectoderm. Its expression overlaps that of *tfap2b* in the diencephalon and rhombencephalon (Fig. 2E-H). These patterns of expression are maintained, with *tfap2b* expression restricted to a subset of *tfap2a*-expressing cells in the pharyngeal ectoderm (Fig. 2I,J). *tfap2a* and *tfap2b* are also

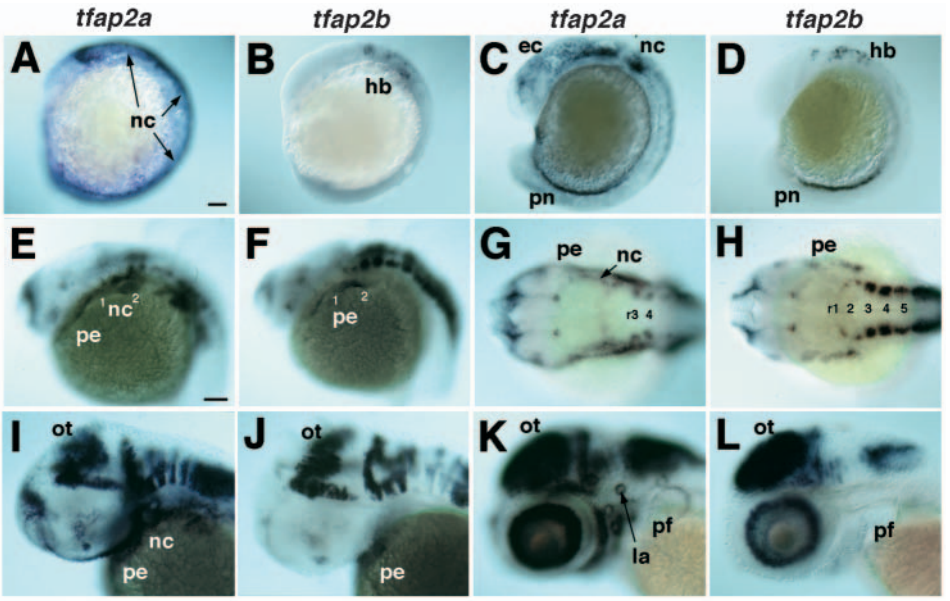

Fig. 2. Expression of *tfap2a* and *tfap2b* in early zebrafish embryos. Whole-mount in situ hybridization was performed with antisense RNA probes. Anterior is towards the left. (A,B) Lateral views at eight somites. (A) Expression of *tfap2a* in neural crest (nc) and non-neural ectoderm. (B) Hindbrain (hb) expression of *tfap2b*. (C,D) Lateral views, 18 somites. (C) *tfap2a* expression in migrating cranial NCCs, non-neural ectoderm (ec) and pronephric duct (pn). (D) *tfap2b* expression in the hindbrain and co-expression with *tfap2a* in the pronephric duct. (E,F) Lateral views of the head at 24 hpf showing co-expression of *tfap2a* and *tfap2b* in the forebrain, and in segmental cell groups in the hindbrain. (E) *tfap2a* expression in the pharyngeal NCCs (nc) and ectoderm (pe). (F) *tfap2b* expression in the ectoderm of arches 1 and 2. (G,H) Dorsal views, 24 hpf. (G) *tfap2a* expression in the CNS, including rhombomeres (r3 and r4) and in pharyngeal NCCs and ectoderm. (H) *tfap2b* expression in rhombomeres of the hindbrain and in pharyngeal ectoderm, but not in NCCs. (I,J) Lateral views, 36 hpf. *tfap2a* and *tfap2b* co-expression in the optic tectum (ot) and tegmentum of the midbrain and hindbrain, and in the pharyngeal ectoderm. Only *tfap2a* is expressed in NCCs. (K,L) Lateral views, 52 hpf. *tfap2a* and *tfap2b* co-expression in the midbrain and hindbrain, and in the ganglion cell layer of the retina. Only *tfap2a* is expressed in the pharyngeal arches, lateral line organs (la) and in the apical ectoderm of the pectoral fins (pf). Scale bars: in A, 100 μm for A-D; in E, 100 μm for E-L.

co-expressed in the lens and retina (ganglion cell layer), midbrain (tectum and tegmentum), cerebellum and spinal cord. These expression domains persist until 52 hpf, whereas, by contrast, *tfap2b* mRNA is no longer detected in the pharyngeal ectoderm after 48 hpf (Fig. 2K,L).

tfap2a and *tfap2b* are both required for craniofacial development

To test *tfap2b* function, 3 ng/embryo of ap2bMO was injected into wild-type embryos at the one- to two-cell stage. This effectively blocked splicing of the *tfap2b* transcript (Fig. 1C) and injected embryos appeared healthy at 72 hpf (Fig. 3A,C). This was also true for injections of 5-10 ng/embryo. By contrast, injection of 3 ng/embryo of ap2bMO into *low* mutants (hereafter referred to as 'AP2a/b-deficient') caused more severe craniofacial defects than *low* alone. In *low* mutants, the jaw hangs ventrally and the hyoid and branchial arches are reduced (Fig. 3B). By contrast, AP2a/b-deficient embryos lack virtually all pharyngeal cartilages (Fig. 3D). *low* mutant embryos were distinguished from ap2bMO-injected wild-type siblings by a lack of melanocytes at 26 hpf. This was further confirmed by PCR identification from tail DNA of ap2bMO-injected mutants using a restriction site created by the *low* lesion in exon 5 of *tfap2a* (data not shown) (Knight et al., 2003).

Closer examination of cartilage confirmed that ap2bMO has no effect in the presence of a functional *tfap2a* gene. In *low* mutants alone, both dorsal (hyosymplectic, hs) and ventral (ceratohyal, ch) hyoid cartilages are reduced, and remnants of the hyoid fuse with the mandibular arch (Fig. 3F). By contrast, AP2a/b-deficient larvae also lack an anterior neurocranium and much of the mandibular arch (Fig. 3H). The posterior neurocranium and pectoral fin skeletons, which are derived from mesoderm, are not affected. Rather, defects are restricted to NCC-derived cartilage, suggesting that *tfap2a* and *tfap2b* play redundant roles in the development of skeletogenic NCCs.

tfap2b is not required for early neural crest cell specification

To determine if *tfap2b*, like *tfap2a*, is required during early NCC development, we examined *dlx2* and *hoxa2* expression in the pharyngeal arches. At 26 hpf, *dlx2* expression marks migrating NCCs in mandibular, hyoid and branchial NCCs (m, h and b in Fig. 4A). *hoxa2* is co-expressed in hyoid and branchial NCCs (Fig. 4D). Both are reduced in the hyoid arch to a few ventral cells in *low* mutants. By contrast, mandibular expression of *dlx2* is unaffected (Fig. 4A,B) (Knight et al., 2003). ap2bMO injections into *low* mutant embryos did not enhance this phenotype (Fig. 4C,F) or disrupt *dlx2* or *hoxa2* expression (data not shown). Thus, unlike *tfap2a*, *tfap2b* is not required for early homeobox gene activation in NCCs.

To test later requirements for *tfap2b* in the arches, we examined expression of the ETS-domain transcription factor *fli1* in AP2a/b-deficient embryos (Brown et al., 2000). *fli1* is first expressed in NCCs at 22 hpf, after migration, and also in vascular endothelia (Fig. 4G-I). In *low* mutants, *fli1* expression is slightly reduced in the hyoid and branchial arches (Fig. 4H), but not in the mandibular arch, similar to *dlx2*. Injection of up to 5 ng of ap2bMO had no effect on *fli1* expression in wild-type controls (data not shown). However, ap2bMO nearly eliminated *fli1* expression in the arches when injected into *low* mutants (Fig 4I). These results are consistent with a requirement for *tfap2b* in NCCs after migration into the arch primordia.

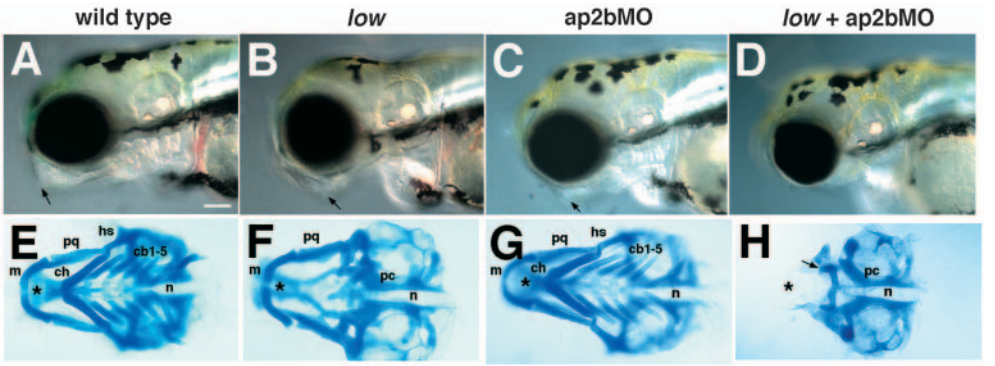

Fig. 3. Jaw and pharyngeal cartilage defects in *low* mutants and in larvae injected with ap2bMO. Lateral views (A-D) of live larvae show reduced head size and jaw defects (arrows) in AP2-deficient animals at 4 dpf. (E-H) Dissected pharyngeal cartilages from 4 dpf shown in ventral view. Pharyngeal cartilages are absent or reduced in all but the mandibular arch in *low* mutants (F), and fuse with the anterior basicranial commissure of the skull. The neurocranium (asterisks) is typically not affected. (G) Injection of ap2bMO alone has no effect, but injection into *low* (H) causes loss of both pharyngeal and neurocranial cartilage. The posterior neurocranium remains intact. cb, ceratobranchial; ch, ceratohyal; hs, hyosymplectic; m, Meckel's cartilage; n, notochord; pc, parachordals; pq, palatoquadrate. Scale bars: 100 μm.

tfap2b regulates patterns of cartilage condensation

To address requirements for *tfap2b* in skeletogenic NCCs, we examined *goosecoid* (*gsc*) and *sox9a* expression (Fig. 4J-O). Both genes play important roles in skeletal differentiation (Rivera-Perez et al., 1999). *gsc* expression is reduced in the dorsal hyoid arch in *low* mutants, and this correlates with loss of *hoxa2* expression and hyosymplectic cartilage. Expression in the ventral arch is unaffected (Fig. 4K) (Knight et al, 2003). Injection of up to 5 ng of ap2bMO has no effect on *gsc* expression (data not shown). However, in AP2a/b-deficient embryos, *gsc* expression is eliminated throughout the hyoid (Fig. 4L). This suggests that *tfap2b* is required for the specification of NCC skeletal progenitors.

Unlike *low/tfap2a*$^{-/-}$ mutants alone, AP2-deficient embryos also show defects in the neurocranium. Two clusters of cartilage precursors in the pharyngeal arches, and a third pair dorsal to the mouth that form the neurocranium, express *sox9a* at 52 hpf (Fig. 4M). *low* mutants lack *sox9a* expression in the hyoid, and mandibular domains remain split at the midline, but do not affect the neurocranium (Fig. 4N). ap2bMO injections alone have no effect on the neurocranium (data not shown), but cause a complete loss of neurocranial *sox9a* expression when injected into *low* (Fig. 4O). These results demonstrate requirements for AP2 function throughout the NCCs that form the neurocranium and pharyngeal arches.

We used a transgenic line in which the *fli1* promotor drives eGFP (*fli1-GFP*), to correlate NCC and skeletal defects (Lawson and Weinstein, 2002). This *fli1-GFP* transgene was crossed into *low*^{ts213} and used to visualize NCCs in the pharyngeal arches of 36 hpf individuals, that were then raised to 4 dpf and stained for cartilage (Fig. 5). In this line, the *fli1-GFP* co-localizes with *dlx2* expression in NCCs (data not shown). *fli1-GFP* expression was reduced in *low* mutants (Fig.

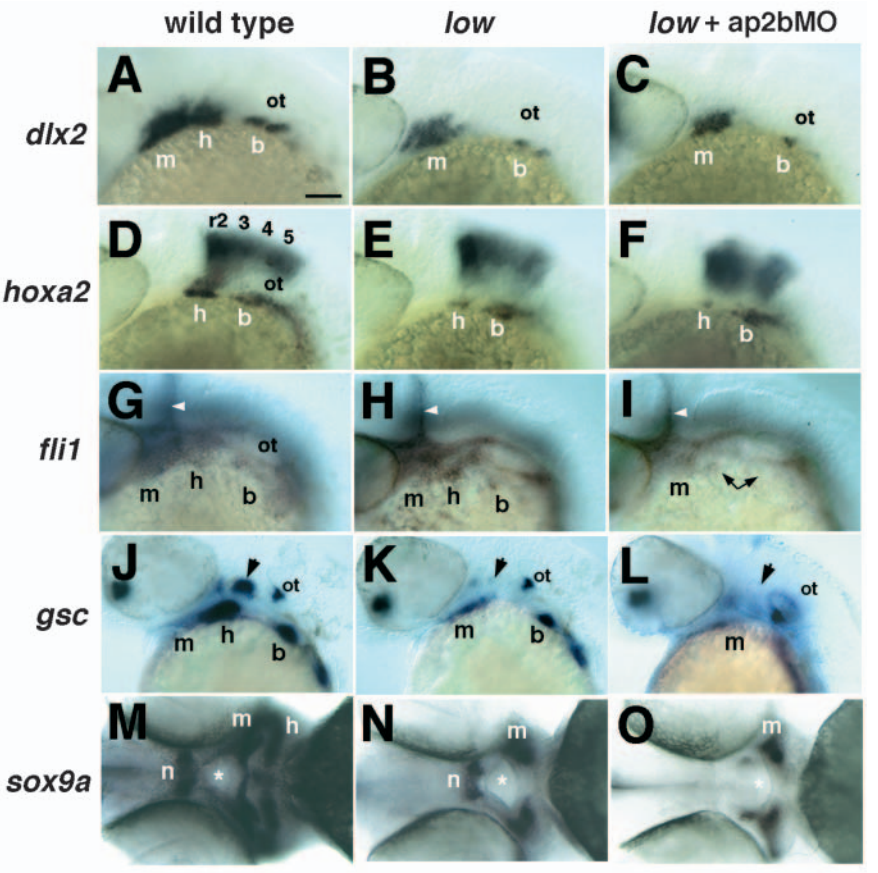

Fig. 4. Defects in pharyngeal arch development in *low* mutants and in larvae injected with ap2bMO. Whole-mount in situ hybridization with riboprobes to *dlx2* (A-C; 28 hpf), *hoxa2* (D-F; 28 hpf), *fli1* (G-I; 28 hpf), *gsc* (J-L; 40 hpf) and *sox9a* (M-O; 52 hpf). (A-L) All embryos are shown in lateral view, except M-O, which are ventral views. Wild-type (A,D,G,J,M), *low* (B,E,H,K,N) and injected *low* mutants (C,F,I,L,O). Arrowheads in G-I indicate vascular expression of *fli1*. Arrows in J-L indicate the hyosymplectic condensation in the dorsal second arch. Asterisks in M-O indicate the mouth. All five NCC markers are reduced in the second pharyngeal arch in *low* mutants, but only *fli1*, *gsc* and *sox9a* defects are enhanced by Tfap2b depletion (L,P,T). b, branchial arches; h, hyoid arch; hb, hindbrain; m, mandibular arch; n, notochord. Scale bars: 100 μm.

5E) and much more severely reduced in AP2a/b-deficient embryos at 36 hpf (Fig. 5F).

We observed a range of defects in *fli1-GFP* expression in *low* mutants and AP2a/b-deficient embryos. Severely affected mutants have weak neurocranial defects (e.g. reduction of the ethmoid plate) and a complete lack of hyoid cartilage, and these correlate with reduced *fli1-GFP* expression in NCCs (Fig. 5E,H). *fli1-GFP* expression persists in the mandibular arch in *low* mutants. By contrast, AP2a/b-deficient embryos lack GFP expression, with only small patches of expression remaining adjacent to the stomodeum and first pharyngeal pouch (Fig. 5F), and these fish completely lack mandibular and neurocranial cartilages (Fig. 5I). These results show that the cartilage defects caused by ap2bMO injection arise in their precursors in postmigratory NCCs.

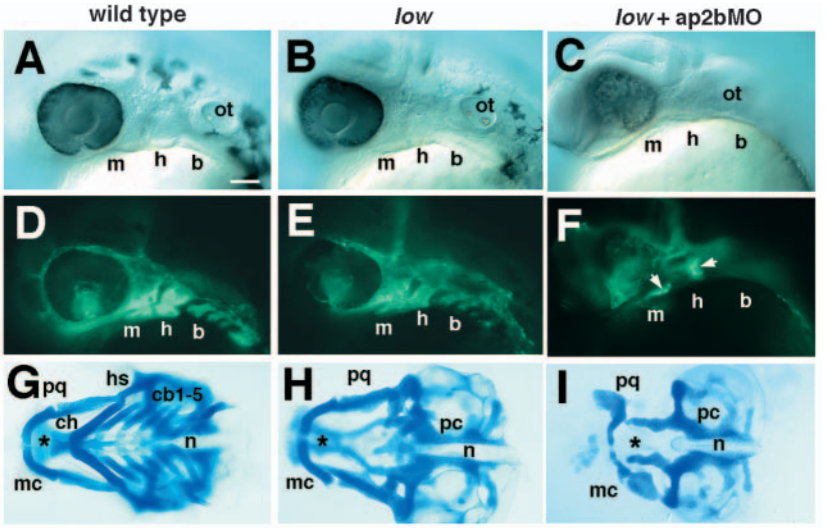

Fig. 5. Cartilage defects correlate with postmigratory NCC defects in *low* mutants and larvae injected with ap2bMO. Columns consist of photos taken at different stages in the same animal. Lateral views of living fli1-GFP transgenic embryos at 28 hpf (A-F) and cartilage preparations from the same individuals at 4 dpf (G-I). *fli1-GFP* expression includes both NCC as well as developing endothelial cells. Arrows in F indicate residual NCCs. b, branchial arches; cb, ceratobranchial; ch, ceratohyal; h, hyoid arch; hs, hyosymplectic; m, mandibular arch; mc, Meckels cartilage; n, notochord; pc, parachordals; pq, palatoquadrate. Scale bars: 100 μm.

tfap2a and *tfap2b* promote survival of pharyngeal ectoderm

tfap2a is required cell autonomously in NCCs (Knight et al., 2003), and in mice Tcfap2a directly regulates *hoxa2* transcription in NCCs (Maconochie et al., 1999). By contrast, zebrafish *tfap2b* is not expressed in NCCs, yet both *tfap2a* and *tfap2b* are required in the NCC-derived skeleton. The only tissue likely to account for this redundancy is the cranial ectoderm, as *tfap2a* is expressed throughout this ectoderm and *tfap2b* is expressed locally in a small patch of pharyngeal ectoderm at 20 hpf. Sections of embryos at both 24 and 36 hpf, labeled by whole-mount in situ hybridization prior to sectioning, reveal that *tfap2a* is expressed in both NCCs and ectoderm (Fig. 6B), and overlaps in NCCs with *dlx2* expression (Fig. 6A). By contrast, *tfap2b* expression is restricted to ectoderm (Fig. 6C). These results suggest that *tfap2b* function is required in the pharyngeal ectoderm, and redundant with that of *tfap2a*.

Do AP2a/b-deficient embryos have defects in pharyngeal ectoderm? AP2 proteins play important roles in cell survival, and *Tcfap2a* mutant mice show elevated apoptosis. We examined apoptosis in the ectoderm using TUNEL labeling (Fig. 7A-I). In the *low*^{ts214} allele of *tfap2a*, a brief period of apoptosis occurs in NCCs between 10 and 14 somites (Knight et al, 2003), and apoptosis is more widespread in the *mob*^{610} allele (Barallo-Gimeno et al., 2004). We performed TUNEL labeling in either *low* mutants alone (Fig. 7B,E,H) or AP2a/b-deficient embryos (Fig. 7C,F,I) carrying the fli1-GFP transgene. Colocalization of GFP and TUNEL showed that apoptosis was excluded from NCCs, and confined to the ectoderm. The number of TUNEL labeled cells in pharyngeal ectoderm at 28 hpf was similar in *low* mutants (4.5±2.62; n=4) and wild-type controls (4.3±2.32; n=6), and only slightly increased in embryos injected with the ap2b MO alone (7.3±4.49; n=5). By contrast, TUNEL labeling was dramatically elevated in AP2a/b-deficient embryos (75.8±16.22; n=6). Large numbers of apoptotic NCCs were observed along the dorsal edges of the spinal cord in the tail, and this correlates with pigment cell defects in the tail in *low* mutants (Fig. 7G-I) (Knight et al, 2004). Elevated ectodermal apoptosis was observed not only in the pharyngeal arches in AP2-deficient animals, but also in olfactory epithelia and in the skin overlying the hindbrain (data not shown).

By contrast, other epithelia such as the pharyngeal endoderm are unaffected by the loss of AP-2. The NK homeobox gene, *nkx2.3*, marks the pharyngeal

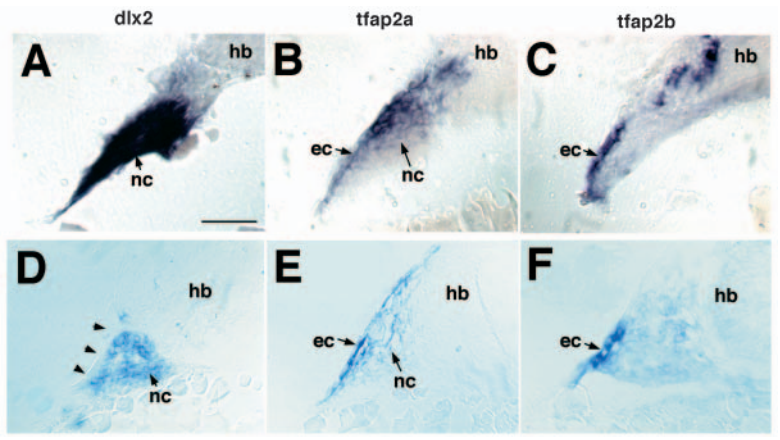

Fig. 6. *tfap2a* and *tfap2b* are co-expressed in the ectoderm, but only *tfap2a* is expressed in pharyngeal arch NCCs. Transverse cryosections through the pharyngeal region of embryos at 26 hpf (A-C) and 36 hpf (D-F) labeled by in situ hybridization with riboprobes to *dlx2* (A,D), *tfap2a* (B,E) and *tfap2b* (C,F). Left side views, with the pharyngeal lumen, neural tube and notochord at the midline lying to the right. Arrowheads in D indicate unlabeled surface ectoderm. Scale bars: 50 μm.

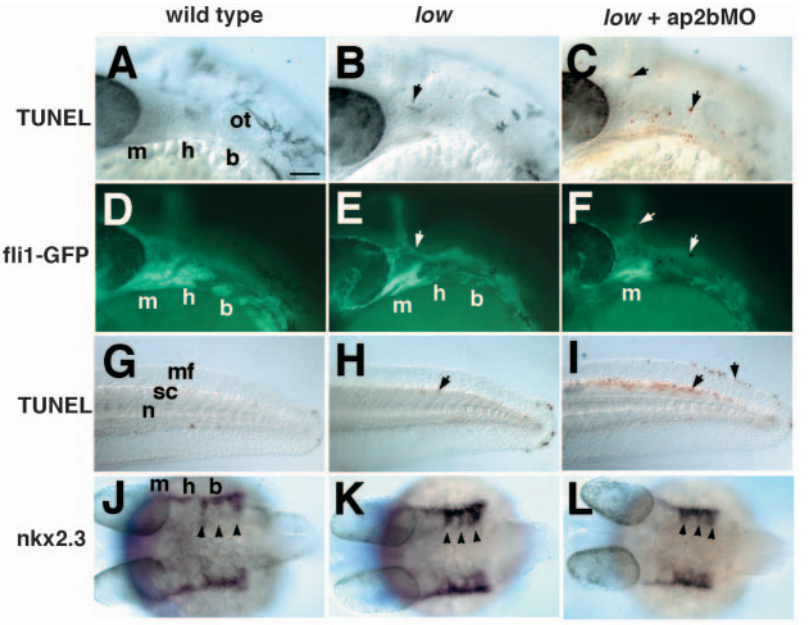

Fig. 7. Defects in ectodermal specification and survival in *low* mutants and in larvae injected with ap2bMO. (A-I) TUNEL labeling of apoptotic cells at 28 hpf is shown in lateral views of the head (A-F) and tail (G-I). (D-F) Co-labeling with TUNEL and the *fli1-GFP* transgene showing apoptosis lateral to the NCCs in the surface ectoderm (arrows). (J-L) In situ hybridization for *nkx2.3* at 28 hpf in dorsal view. Expression is detected in pharyngeal ectoderm and endodermal pouches (arrowheads). b, branchial; h, hyoid; m, mandibular; mf, median fin; n, notochord; ot, otic vesicle; sc, spinal cord. Scale bars: 100 μm.

pouch endoderm at 34 hpf (Fig. 7J), and this endoderm forms a normal series of pouches in *low* mutants and in AP2a/b-deficient embryos (Fig. 7K,L).

Ectodermal grafts rescue AP2-dependent cartilages

To determine if *tfap2a* and *tfap2b* are required in ectoderm, we performed transplants. Ectodermal precursors were transplanted at blastula stages, from fluorescently labeled wild-type donor embryos [injected with tetramethylrhodamine (TRITC) and biotin-conjugated dextrans], into unlabeled *low* mutants injected with ap2bMO (Fig. 8A). Cells placed near the animal pole gave rise to scattered clones in the skin of the head at later stages. Transplanted cells contributed to the olfactory epithelia (n=34; Fig. 8E), retina (n=36; Fig. 8F,G) and neural tube (n=6), as well as the pharyngeal ectoderm (n=14; Fig. 8E-G), but not to the mesoderm or endoderm. Of 14 *low* mutant hosts with transplanted wild-type pharyngeal ectoderm, four showed unilateral rescue of hyoid arch development coinciding with the transplanted cells (Fig. 8, left and center columns). Similar rescues were achieved in 5/9 transplants of pharyngeal ectoderm into *low* mutants injected with ap2bMO (Fig. 8, right

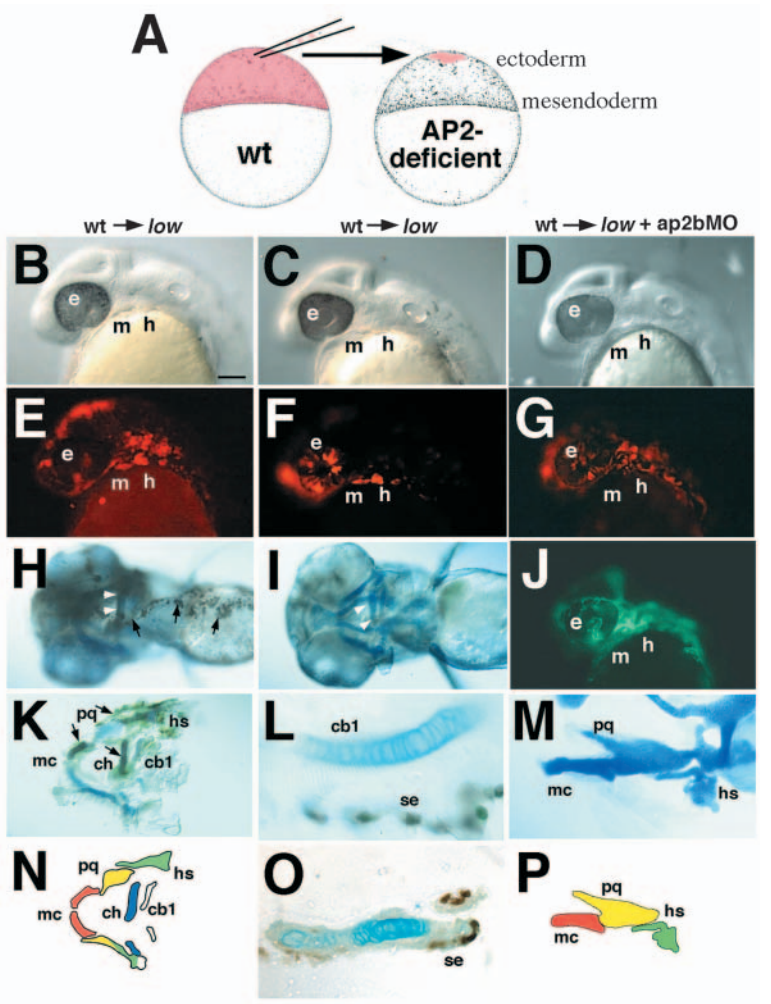

Fig. 8. Transplants suggest that *tfap2a* and *tfap2b* are required in the pharyngeal ectoderm, and act non-autonomously in NCCs. Each column represents photos taken at different stages of the same animal. Columns 1 and 2 show transplants from wild-type donors into *low* mutant hosts, whereas the host in column 3 is a *low* mutant injected with ap2bMO. Prospective cranial ectodermal cells were transplanted from donor embryos labeled with a lineage tracer into unlabeled hosts at 4-5 hpf (A). Lateral views of living mosaic embryos at 28 hpf (A-G) showing that transplanted cells (red rhodamine-labeled cells in E-G) form patches of ectoderm covering parts of the face and arches. (H,I) Ventral views of mosaic larvae at 4 dpf stained for biotinylated lineage tracer (brown) in the ectoderm. Arrows in H indicate transplanted donor cells in ectoderm. Arrowheads in H,I indicate rescued cartilage of the ceratohyal. (J) fli1-GFP expression in the same embryo as G. (K,M) Flat-mounted rescued cartilages (blue) with ectoderm attached (brown). (L) Higher magnification view of the larvae shown in I, in which transplanted ectodermal cells and cartilage can be clearly distinguished. (O) Section through rescued ceratohyal cartilage in K. (N,P) Diagrams of cartilages shown in K and M. cb, ceratobranchial; ch, ceratohyal; e, ethmoid; h, hyoid arch; hs, hyosymplectic; m, mandibular arch; mc, Meckel's cartilage; ot, otic vesicle; pc, parachordals; pq, palatoquadrate; se, surface ectoderm; t, trabeculae. Scale bars: 50 μm.

column), and in these cases we also observed rescue of *fli1-GFP* expression on the transplanted side (Fig. 8J). Transplanted cells were clearly situated in the ectoderm when TRITC was compared with *fli1-GFP* (compare Fig. 8G and 8J) and later biotin-labeling compared with cartilage at 4 dpf (Fig. 8H,I). In each case, either the ceratohyal, hyosymplectic or ceratobranchial cartilages (or in some cases all three) were rescued on one side adjacent to transplanted ectodermal cells (Fig. 8K-P). In some cases, transplants also rescued more dorsal defects in the neurocranium, indicating that the ectoderm also influences these cartilages. This demonstrates that *tfap2a* and *tfap2b* are required non-autonomously in the ectoderm to regulate NCC-derived cartilage differentiation, in addition to the well-documented, cell-autonomous roles of *tfap2a* in NCCs.

AP2 regulates Fgf signaling from the ectoderm

What ectodermal signal is disrupted in AP2a/b-deficient embryos? Shh, Bmp4 and Fgf8 are expressed in the facial ectoderm, and all three have been implicated in NCC patterning, proliferation and survival (Bachler and Neubeuser, 2001). *tfap2a* mutants lack Shh expression in the posterior ectoderm of the hyoid arch (Knight et al., 2003), but injection of ap2b-MO into *low* mutants does not cause any defects in *shh* expression. Likewise, *bmp4* expression is only slightly reduced in the ventral ectoderm in AP2a/b-deficient embryos (data not shown). To address requirements for AP-2 in regulating Fgfs, we examined *fgf3* and *fgf8* expression, both of which have been implicated in craniofacial development in zebrafish (Roehl and Nusslein-Volhard, 2001; David et al., 2002). *fgf8* is expressed in the mandibular ectoderm and more weakly in more posterior arch ectoderm at 28 hpf. Expression of both *fgf3* and *fgf8* persists in AP2a/b-deficient embryos (Fig. 9A,B).

Other Fgf proteins (Fgf9, Fgf17 and Fgf18) expressed in cranial ectoderm in mammals have not been well characterized in zebrafish. Therefore, we examined expression of the interleukin receptor-related Fgf target *sef* as a general indicator of responses to Fgfs in the arches. *sef* is expressed in cranial NCCs in the arches beginning at 18 hpf, and near other sources of Fgfs at the mid-hindbrain boundary and in the pectoral fin buds (Fig. 9C). Expression of *sef* is lost in the first arch (mandibular) and strongly reduced in the second arch (hyoid) in AP2a/b-deficient embryos, while other domains of expression are unaffected (Fig. 9D). This appears to reflect a loss of Fgf produced by the ectoderm, as transplantation of wild-type pharyngeal ectoderm partially rescues *sef* expression on the grafted side (8/18; Fig. 9E). Our results implicate Fgfs as one component of the ectodermal signals that require the combined functions of Tfap2a and Tfap2b.

Discussion

We have identified a zebrafish *tfap2b* required for craniofacial development that acts together with *tfap2a* in the pharyngeal ectoderm to promote skeletal development of NCCs. Two lines of evidence lead to these conclusions: (1) *tfap2b* is expressed in the ectoderm, but not in NCCs, yet it functions redundantly with *tfap2a* in cartilage development; (2) transplantation of wild type ectoderm into an AP2a/b-deficient embryo partially rescues NCC-derived cartilage. Based on our morpholino

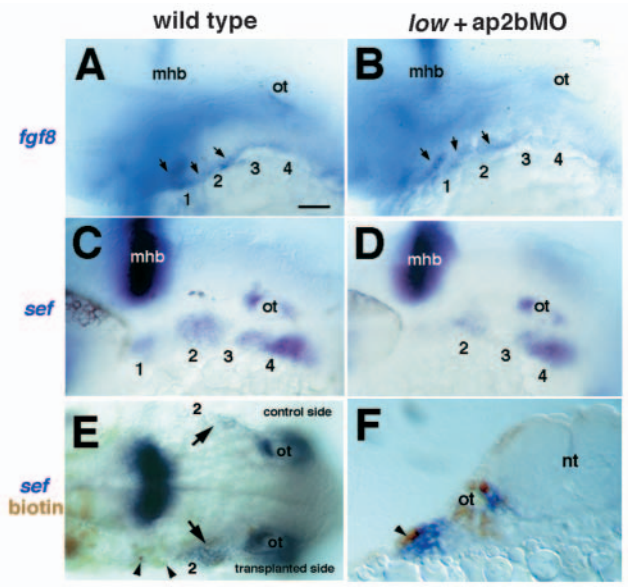

Fig. 9. *tfap2a* and *tfap2b* are required for Fgf signaling in NCCs. Lateral views, anterior towards the left. (A,B) At 32 hpf, *fgf8* mRNA is detected in wild type in the ectoderm covering the arches, in addition to the mid-hindbrain boundary (mhb); this expression remains in AP2a/b-deficient embryos. Arrows in A,B indicate ectodermal expression of *fgf8*. (C,D) At 28 hpf in wild type, *sef* mRNA is detected in NCCs; this expression is severely reduced in AP2a/b-deficient embryos. (E,F) Mosaic embryos in which biotin-labeled, wild-type ectodermal cells (brown, arrows) were transplanted on one side of the head and partially restore *sef* expression (blue). (E) Dorsal view, anterior towards the left showing transplanted side with substantially increased levels of sef expression, and lack of expression on the contralateral, control side (arrows). (F) A transverse section through the embryo shown in E at the level of the hyoid arch showing grafted wild-type ectoderm (brown) and rescued *sef* expression in underlying NC (blue). Arrowhead in F indicates transplanted ectoderm. m, mandibular arch; h, hyoid arch; b, branchial arches. Scale bars: 50 μm.

studies, *tfap2b* is not required for early NCC specification, but only later after migration. We propose that AP2 genes act in two separate aspects of NCC development (Fig. 10). First, *tfap2a* regulates specification of skeletal precursor cells and their segmental identities, through regulation of Hox group 2 genes (Knight et al., 2003). Second, *tfap2a* and *tfap2b* together control Fgfs and perhaps other signals from the ectoderm that regulate skeletogenesis. The coordinated action of these pathways mediates the spatiotemporal formation of craniofacial cartilage and bone.

Redundancies between *tfap2a* and *tfap2b*

In mice, *Tcfap2a* and *Tcfap2b* are co-expressed in many embryonic tissues such as NCCs, yet have unique requirements in development. Loss-of-function mutations in *Tcfap2a* disrupt neural tube closure and craniofacial NCCs (Schorle et al., 1996; Zhang et al., 1996). By contrast, mutations in *Tcfap2b* or human *TFAP2B*, cause renal failure and craniofacial defects associated with Char syndrome (Moser et al., 1997b; Satoda et al., 2000). AP2 proteins may function redundantly in tissues where they are co-expressed, and our results support this hypothesis for the ectoderm (Moser et al., 1997a). Zebrafish

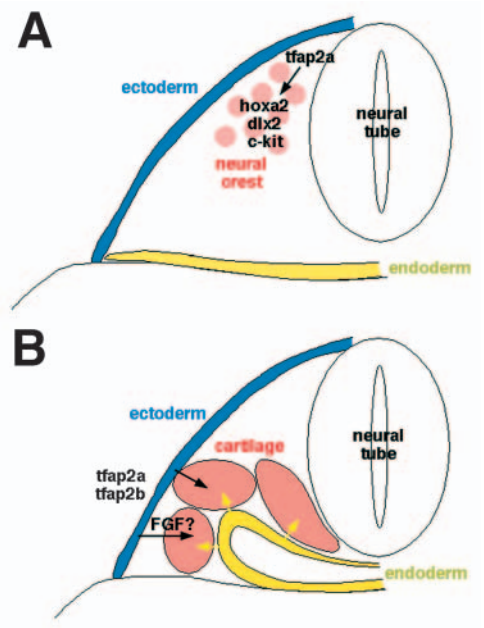

Fig. 10. Model depicting proposed cell autonomous and non-autonomous roles for AP2 proteins in NCC development. Illustrations of transverse sections depicting early migratory stages of NCCs (A) and later interactions within the pharyngeal primordia (B). (A) Initially, *tfap2a* acts autonomously within NCCs to regulate *hoxa2*, *dlx2* and *kit* expression. (B) Later, *tfap2a* and *tfap2b* act together in the surface ectoderm (blue) to regulate Fgf8 and possibly other Fgfs that activate *sef* expression and control cartilage development, together with Fgf3 signaling from the pharyngeal endoderm (yellow).

tfap2b is only co-expressed with *tfap2a* in a restricted domain within the pharyngeal ectoderm. Few studies have addressed AP2 functions in ectoderm as the skin appears to develop normally in *Tfap2a*$^{-/-}$ and *Tfap2b*$^{-/-}$ mutant mice (Schorle et al., 1996). Disruption of *tfap2b* alone has no effect on zebrafish embryos, but enhances defects in ectodermal cell survival and craniofacial cartilage caused by loss of *tfap2a* alone, suggesting that the two AP2 proteins can compensate for one another. *tfap2a* and *tfap2b* are also co-expressed in the pronephric ducts, and in several regions of the CNS, where they may also be redundant.

Separate requirements for AP2 genes in early versus late NCC development

tfap2a promotes *Hoxa2* expression in NCCs that populate the hyoid arch (Maconochie et al., 1999; Knight et al., 2003; Knight et al., 2004). *hoxa2* expression may similarly be activated by *tfap2b*, which shares nearly identical DNA-binding domains and binds a NCC-specific *Hoxa2* enhancer, albeit with different affinity (Maconochie et al., 1999). To address this issue in NCCs, we morpholino-depleted *tfap2b* from *low* (*tfap2a*) mutants, examined *hoxa2* mRNA, and found that the loss of *tfap2b* had no effect. This suggests that *tfap2b* does not compensate for *tfap2a* in activating *hoxa2*, but only later in cartilage induction. Our data also argue against a role for AP2 genes in NCC migration. NCCs migrate into all of the arches in the *low* allele of *tfap2a* (Knight et al., 2003), though some cells fail to migrate into the hyoid arch in the *mob610* allele (Barrallo-Gimeno et al., 2004) and we show that depletion of Tfap2b protein in *low* does not enhance defects in early markers of migrating NCCs such as *hoxa2* and *dlx2*.

Rather, we argue that *tfap2b* regulates NCC specification after migration into the arches as cells condense to form cartilage. In contrast to *hoxa2*, expression of *fli1* is reduced in AP2a/b-deficient embryos, compared with *low* alone, and we used a fli1-GFP transgene to show that this prefigures condensation defects. Later markers of differentiating cartilage, such as *gsc* and *sox9a*, are almost completely eliminated in these embryos. Surprisingly, AP2a/b-deficient embryos also have defects in the neurocranium. As both pharyngeal and neurocranial cartilages derive from NCCs (the posterior head skeleton is mesodermal) these results suggest that AP2 genes are required for the development of other NCC-derived cartilages. *tfpa2a* and *tfap2b* may be partially redundant in more anterior cartilages of the mandibular arch and neurocranium, which are not disrupted in *tfap2a*$^{-/-}$ mutants alone.

Separate requirements for AP2 genes in NCCs and in surface ectoderm

Tcfap2a is required cell-autonomously for NCC specification, prior to migration into the pharyngeal arches (Knight et al., 2003; Knight et al., 2004), and directly regulates *hoxa2* and *kit* transcription (Maconochie et al., 1999). Here, we show an additional non-autonomous requirement for AP2 proteins in the pharyngeal ectoderm. To achieve this, we grafted ectodermal precursors from wild-type donors into either *low* or AP2a/b-deficient embryos and analyzed the cartilage pattern. Grafts that included pharyngeal ectoderm rescued cartilage unilaterally on the transplanted side, including restoration of dorsal first (palatoquadrate) and second (hyosymplectic) arch cartilages, as well as their separation from the neurocranium. This is a dramatic example of a non-autonomous role for ectoderm in cartilage development and is consistent with previous studies in mice implicating the surface ectoderm in arch patterning (Trumpp et al., 1999; Trokovic et al., 2003; Macatee et al., 2003). A non-autonomous requirement for *tfap2a* has previously been suggested for NCC-derived melanocytes (O'Brien et al., 2004). These requirements in ectoderm appear to act separately and in parallel to chondrogenic signals from the pharyngeal endoderm (Hall, 1980; David et al., 2002), and AP2-deficient embryos show no defects in endoderm.

Ectodermal signals may also regulate Hox gene expression in the arches and arch identities. Cartilage defects in *low* (*tfap2a*) mutant zebrafish resemble homeotic defects caused by loss of Hox group 2 gene function, in which hyoid cartilages are transformed to a mandibular fate (Knight et al., 2004). This could be caused directly by loss of *Hoxa2* transcriptional activation by AP2 proteins in NCCs, or indirectly by defects in surrounding tissues. Our results indicate both direct and indirect roles for *tfap2a*, as ectodermal grafts rescue cartilage formation as well as homeotic transformations of the hyoid skeleton in *low* mutant embryos (Knight et al., 2004). This suggests that Hox genes initially specify the segmental identities of migrating NCCs, but then require ectodermal signals to maintain this identity (Trainor and Krumlauf, 2000; Schilling et al., 2000). Defects in *Hoxa2*$^{-/-}$ mutant mice have

been interpreted as intrinsic changes in NCC, but *Hoxa2* expression is lost in both ectoderm and NCCs, and the role of the ectoderm has been largely ignored. In Hoxa2 mutants, ectopic expression of mandibular arch genes in the hyoid arch results from defects in reciprocal signals between NCCs and ectoderm (Bobola et al., 2003). Our results suggest that the ectoderm maintains Hox expression in NCCs during migration, and this depends on AP2 genes.

Tcfap2a expression begins during gastrulation in the non-neural ectoderm and persists in the skin throughout embryonic development. We show that AP2-deficient zebrafish have defects in ectodermal survival. *Tcfap2a* promotes ectoderm formation in *Xenopus* (Luo et al., 2002; Luo et al., 2003) and regulates genes involved in epidermal differentiation in mammals (Pfisterer et al, 2002; Zhang et al, 1996; Schorle et al, 1996). In contrast to *tfap2a*, however, which is expressed broadly in the ectoderm, *tfap2b* expression is restricted to the pharyngeal ectoderm, and it is here that we find elevated apoptosis by TUNEL labeling in AP2a/b-deficient embryos. We previously described a wave of early apoptosis in the premigratory NCCs and overlying ectoderm in *low* mutants at neurula stages (Knight et al., 2003) and death is even more extensive in the pharyngeal arches of the *mob610* allele of *tfap2a* (Barrallo-Gimeno et al., 2004). Apoptosis in the NCCs is considered to be the causative phenotype for mouse *Tcfap2a* mutants, implying that AP2 genes function cell-autonomously in NCC survival (Hilger-Eversheim et al., 2000; Decary et al., 2002), but we have not observed extensive death in NCCs in AP2-deficient zebrafish, only ectoderm.

AP2, Hoxa2 and Fgf signaling

Many growth factors (e.g. Fgf8, Shh, Bmp4, etc.) are expressed in pharyngeal ectoderm and have been implicated in craniofacial development (Wall and Hogan, 1995). Our results suggest that one component of the ectodermal signal to NCCs is an Fgf, but probably not Fgf8. Expression of the Fgf-responsive gene *sef*, is disrupted in AP2a/b-deficient embryos, and can be partially rescued by grafts of wild-type ectoderm. Several Fgfs are expressed in the pharyngeal ectoderm, including Fgf8 and Fgf17 (Reifers et al., 2000). However, *fgf8* mRNA appears unaffected in AP2a/b-deficient zebrafish embryos. We have previously shown that *tfap2a* is also required for *shh* expression in the posterior ectodermal margin of the hyoid arch (Knight et al., 2004). Thus, in the hyoid arch, AP2 proteins may simultaneously regulate Shh and Fgf signals from the pharyngeal ectoderm that control skeletal growth and pattern.

Fgf8 seemed the most likely candidate to be regulated in the ectoderm, because it is required for mandibular development in the mouse (Trumpp et al., 1999; Abu-Issa et al., 2002). Macatee et al. (Macatee et al., 2003) used Cre-lox mediated removal of *Fgf8* in the pharyngeal ectoderm to demonstrate an ectodermal requirement in mice. These animals lacked mandibular arches and more posterior arches were fused. By contrast, *fgf3* is required in the endoderm for formation of the posterior, branchial arch skeleton, but appears to play less of a role in the mandibular and hyoid (David et al., 2002) and we have not detected any defects in *fgf3* expression in AP2a/b-deficient embryos. Both *fgf3* and *fgf8* in zebrafish play a role in endodermal pouch formation, and the combined disruption of both leads to severe reductions in the cranial skeleton (Walshe and Mason, 2003; Crump et al., 2004). Likewise, a hypomorphic mutation in *Fgfr1* in the facial ectoderm in mice eliminates the hyoid arch skeleton but not the mandibular arch, similar to *low*/*tfap2a* mutant zebrafish (Trokovic et al., 2003), suggesting that Fgfs expressed in the ectoderm autoregulate their own expression and subsequent signaling to adjacent NCCs.

Interestingly, Fgf signaling in the mouse has been proposed to inhibit *Hoxa2* expression in mandibular arch NCCs, suggesting that this may be a convergence point for AP2 and Fgf functions in establishing pharyngeal arch identity. *Hoxa2* represses Fgf activated genes such as *Pitx1* and *Lhx6* in NCCs of the hyoid arch (Bobola et al., 2003). In *Hoxa2*$^{-/-}$ mutants, these genes are ectopically expressed and the hyoid arch is transformed to a mandibular fate. We previously described similar transformations in *low* mutant zebrafish. Our data suggest that these are due to an early function for *tfap2a* in regulating the expression of *hoxa2* directly in NCCs, while a *tfap2b*-dependent signal from the ectoderm (possibly an Fgf) is involved only later in chondrogenesis.

Conserved functions for AP2 transcription factors in vertebrate development

NCCs arose at the origin of vertebrates and many of the genes involved in NCC patterning evolved from ancestral genes that had more ancient roles in patterning other tissues. In the invertebrate chordate, amphioxus, an AP2 gene is expressed in the non-neural ectoderm, indicating that this is a conserved feature of AP2 genes in all chordates (Meulemans and Bronner-Fraser, 2002). Pharyngeal arches also have an origin prior to that of the NCCs, as evidenced by the presence of branchial gills in amphioxus and appendicularian urochordates. The pharyngeal arches are initially patterned independently of NCCs as shown by NCC extirpations in the chick, in which ectodermal and endodermal patterning is not perturbed (Veitch et al., 1999). Given that AP2 genes have ancient roles in patterning of the ectoderm and that pharyngeal arches arose prior to the NCCs, it is tempting to speculate that AP2 genes were involved in patterning the pharyngeal ectoderm prior to the origin of NCCs. Thus, when NCCs first gained their migratory behavior, they retained some of their identity from their site of origin in the hindbrain through NCC-specific genes, such as *tfap2a*, but were influenced by signals already present in the arch environment into which they migrated, including those regulated by AP2.

We thank T. Williams and I. Blitz for stimulating discussions, as well as K. Cho, I. Blitz, and members of our laboratory for critical reading of the manuscript. We also thank B. Weinstein for the kind gift of the fli1-GFP transgenic strain and the following people for fish and probes: C. Kimmel, V. Prince and D. Stemple. This work was supported by the NIH (NS-41353, DE-13828), March of Dimes (1-FY01-198) and Pew Scholars Foundation (2615SC) to T.S.

References

Abu-Issa, R., Smyth, G., Smoak, I., Yamamura, K. and Meyers, E. N. (2002). Fgf8 is required for pharyngeal arch and cardiovascular development in the mouse. *Development* **129**, 4613-4625.

Akimenko, M. A., Ekker, M., Wegner, J., Lin, W. and Westerfield, M. (1994). Combinatorial expression of three zebrafish genes related to distal-less: part of the homeobox gene code for the head. *J. Neurosci.* **14**, 3475-3486.

Auman, H. J., Nottoli, T., Lakiza, O., Winger, Q., Donaldson, S. and Williams, T. (2002). Transcription factor AP-2gamma is essential in the extra-embryonic lineages for early postimplantation development. *Development* **129**, 2733-2747.

Bachler, M. and Neubuser, A. (2001). Expression of members of the Fgf family and their receptors during midfacial development. *Mech. Dev.* **100**, 313-316.

Barrallo-Gimeno, A., Holzschuh, J., Driever, W. and Knapik, E. W. (2004). Neural crest survival and differentiation in zebrafish depends on mont blanc/tfap2a gene function. *Development* **131**, 1463-1477.

Bobola, N., Carapuco, M., Ohnemus, S., Kanzler, B., Leibbrandt, A., Neubuser, A., Drouin, J. and Mallo, M. (2003). Mesenchymal patterning by Hoxa2 requires blocking Fgf-dependent activation of Ptx1. *Development* **130**, 3403-3414.

Brown, L. A., Rodaway, A. R., Schilling, T. F., Jowett, T., Ingham, P. W., Patient, R. K. and Sharrocks, A. D. (2000). Insights into early vasculogenesis revealed by expression of the ETS-domain transcription factor Fli-1 in wild-type and mutant zebrafish embryos. *Mech. Dev.* **90**, 237-252.

Chazaud, C., OuladAbdelghani, M., Bouillet, P., Decimo, D., Chambon, P. and Dolle, P. (1996). AP-2.2, a novel gene related to AP-2, is expressed in the forebrain, limbs and face during mouse embryogenesis. *Mech. Dev.* **54**, 83-94.

Creuzet, S., Schuler, B., Couly, G. and LeDouarin, N. M. (2004). Reciprocal relationships between Fgf8 and neural crest cells in facial and forebrain development. *Proc. Natl. Acad. Sci. USA* **101**, 4843-4847.

Crump, J. G., Maves, L., Lawson, N. D., Weinstein, B. M. and Kimmel, C. B. (2004). An essential role for Fgfs and endodermal pouch formation influences later craniofacial skeletal patterning. *Development* **131**, 5703-5716.

David, N. B., Saint-Etienne, L., Tsang, M., Schilling, T. F. and Rosa, F. M. (2002). Requirement for endoderm and FGF3 in ventral head skeleton formation. *Development* **129**, 4457-4468.

Decary, S., Decesse, J. T., Ogryzko, V., Reed, J. C., Naguibneva, I., Harel-Bellan, A. and Cremisi, C. E. (2002). The retinoblastoma protein binds the promoter of the survival gene bcl-2 and regulates its transcription in epithelial cells through transcription factor AP-2. *Mol. Cell. Biol.* **22**, 7877-7888.

Furthauer, M., Thisse, C. and Thisse, B. (1997). A role for FGF-8 in the dorsoventral patterning of the zebrafish gastrula. *Development* **124**, 4253-4264.

Furthauer, M., Lin, W., Ang, S. L., Thisse, B. and Thisse, C. (2002). Sef is a feedback-induced antagonist of Ras/MAPK-mediated Fgf signaling. *Nat. Cell Biol.* **4**, 170-174.

Graham, A. (2003). Development of the pharyngeal arches. *Am. J. Med. Genet.* **119A**, 251-256.

Hall, B. K. (1980). Tissue interactions and the initiation of osteogenesis and chondrogenesis in the neural crest-derived mandibular skeleton of the embryonic mouse as seen in isolated murine tissues and in recombinations of murine and avian tissues. *J. Embryol. Exp. Morph.* **58**, 251-264.

Hilger-Eversheim, K., Moser, M., Schorle, H. and Buettner, R. (2000). Regulatory roles of AP-2 transcription factors in vertebrate development, apoptosis and cell cycle control. *Gene* **260**, 1-12.

Hu, D. and Helms, J. A. (1999). The role of sonic hedgehog in normal and abnormal craniofacial morphogenesis. *Development* **126**, 4873-4884.

Huang, S., Jean, D., Luca, M., Tainsky, M. A. and Bar-Eli, M. (1998). Loss of AP-2 results in downregulation of c-KIT and enhancement of melanoma tumorigenicity and metastasis. *EMBO J.* **17**, 4358-4369.

Hunter, M. P. and Prince, V. E. (2002). Zebrafish hox paralogue group 2 genes function redundantly as selector genes to pattern the second pharyngeal arch. *Dev. Biol.* **247**, 367-389.

Javidan, Y. and Schilling, T. F. (2004). Development of cartilage and bone. In *Methods in Cell Biology: Zebrafish Biology* (ed. H. W. Detrich, M. Westerfield and L. I. Zon), pp. 415-436. London: Academic Press.

Jeong, J., Mao, J., Tenzen, T., Kottmann, A. H. and McMahon, A. P. (2004). Hedgehog signaling in neural crest cells regulates the patterning and growth of facial primordia. *Genes Dev.* **18**, 937-951.

Kettunen, P. and Thesleff, I. (1998). Expression and function of FGFs-4, -8, and -9 suggest functional redundancy and repetitive use as epithelial signals during tooth morphogenesis. *Dev. Dyn.* **211**, 256-268.

Kimmel, C. B., Warga, R. M. and Schilling, T. F. (1990). Origin and organization of the zebrafish fate map. *Development* **108**, 581-594.

Kimmel, C. B., Ballard, W. W., Kimmel, S. R., Ullmann, B. and Schilling, T. F. (1995). Stages of embryonic development of the zebrafish. *Dev. Dyn.* **203**, 253-310.

Kimmel, C. B., Miller, C. T., Kruze, G., Ullmann, B., BreMiller, R. A., Larison, K. D. and Snyder, H. C. (1998). The shaping of pharyngeal cartilages during early development of the zebrafish. *Dev. Biol.* **203**, 245-263.

Knight, R. D., Nair, S., Nelson, S. S., Afshar, A., Javidan, Y., Geisler, R., Rauch, G. J. and Schilling, T. F. (2003). Lockjaw encodes a zebrafish tfap2a required for early neural crest development. *Development* **130**, 5755-5768.

Knight, R. D., Javidan, Y., Nelson, S., Zhang, T. and Schilling, T. F. (2004). Skeletal and pigment cell defects in the lockjaw mutant reveal multiple roles for zebrafish *tfap2a* in neural crest development. *Dev. Dyn.* **229**, 87-98.

Lawson, N. D. and Weinstein, B. M. (2002). In vivo imaging of embryonic vascular development using transgenic zebrafish. *Dev. Biol.* **248**, 307-318.

Leask, A., Byrne, C. and Fuchs, E. (2001). Transcription factor AP2 and its role in epidermal-specific gene expression. *Proc. Natl. Acad. Sci. USA* **88**, 7948-7952.

Lee, K. H., Xu, Q. and Breitbart, R. E. (1996). A new tinman-related gene, nkx2.7, anticipates the expression of nkx2.5 and nkx2.3 in zebrafish heart and pharyngeal endoderm. *Dev. Biol.* **180**, 722-731.

Li, M., Zhao, C., Wang, Y., Zhao, Z. and Meng, A. (2002). Zebrafish *sox9b* is an early neural crest marker. *Dev. Genes Evol.* **212**, 203-206.

Luo, T., Matsuo-Takasaki, M., Thomas, M. L., Weeks, D. L. and Sargent, T. D. (2002). Transcription factor AP-2 is an essential and direct regulator of epidermal development in Xenopus. *Dev. Biol.* **245**, 136-144.

Luo, T., Lee, Y. H., Saint-Jeannet, J. P. and Sargent, T. D. (2003). Induction of neural crest in Xenopus by transcription factor AP-2 alpha. *Proc. Natl. Acad. Sci. USA* **100**, 532-537.

Maconochie, M., Krishnamurthy, R., Nonchev, S., Meier, P., Manzanares, M., Mitchell, P. J. and Krumlauf, R. (1999). Regulation of Hoxa2 in cranial neural crest cells involves members of the AP-2 family. *Development* **126**, 1483-1494.

Macatee, T. L., Hammond, B. P., Arenkiel, B. R., Francis, L., Frank, D. U. and Moon, A. M. (2003). Ablation of specific expression domains reveals discrete functions of ectoderm- and endoderm-derived FGF8 during cardiovascular and pharyngeal development. *Development* **130**, 6361-6374.

Meulemans, D. and Bronner-Fraser, M. (2002). Amphioxus and lamprey AP-2 genes: implications for neural crest evolution and migration patterns. *Development* **129**, 4953-4962.

Morriss-Kay, G. M. (1996). Craniofacial defects in AP-2 null mutant mice. *BioEssays* **18**, 785-788.

Moser, M., Imhof, A., Pscherer, A., Bauer, R., Amselgruber, W., Sinowatz, F., Hofstadter, F., Schule, R. and Buettner, R. (1995). Cloning and characterization of a second AP-2 transcription factor: AP-2 beta. *Development* **121**, 2779-2788.

Moser, M., Ruschoff, J. and Buettner, R. (1997a). Comparative analysis of AP-2 alpha and AP-2 beta gene expression during murine embryogenesis. *Dev. Dyn.* **208**, 115-124.

Moser, M., Pscherer, A., Roth, C., Becker, J., Mucher, G., Zerres, K., Dixkens, C., Weis, J., Guay-Woodford, L., Buettner, R. et al. (1997b). Enhanced apoptotic cell death of renal epithelial cells in mice lacking transcription factor AP-2beta. *Genes Dev.* **11**, 1938-1948.

O'Brien, E. K., d'Alencon, C., Bonde, G., Li, W., Schoenebeck, J., Allende, M. L., Gelb, B. D., Yelon, D., Eisen, J. S. and Cornell, R. A. (2004). Transcription factor Ap-2alpha is necessary for development of embryonic melanophores, autonomic neurons and pharyngeal skeleton in zebrafish. *Dev. Biol.* **265**, 246-261.

Pfisterer, P., Ehlermann, J., Hegen, M. and Schorle, H. (2002). A subtractive gene expression screen suggests a role of transcription factor AP-2 alpha in control of proliferation and differentiation. *J. Biol. Chem.* **277**, 6637-6644.

Prince, V. E., Moens, C. B., Kimmel, C. B. and Ho, R. K. (1998). Zebrafish hox genes: expression in the hindbrain region of wild-type and mutants of the segmentation gene, valentino. *Development* **125**, 393-406.

Reifers, F., Adams, J., Mason, I. J., Schulte-Merker, S. and Brand, M. (2000). Overlapping and distinct functions provided by fgf17, a new zebrafish member of the Fgf8/17/18 subgroup of Fgfs. *Mech. Dev.* **99**, 39-49.

Rivera-Perez, J. A., Wakamiya, M. and Behringer, R. R. (1999). Goosecoid acts cell autonomously in mesenchyme-derived tissues during craniofacial development. *Development* **126**, 3811-3821.

Roehl, H. and Nusslein-Volhard, C. (2001). Zebrafish pea3 and erm are general targets of FGF8 signaling. *Curr. Biol.* **11**, 503-507.

Santagati, F. and Rijli, F. M. (2003). Cranial neural crest and the building of the vertebrate head. *Nat. Rev. Neurosci.* **4**, 806-818.

Satoda, M., Zhao, F., Diaz, G. A., Burn, J., Goodship, J., Davidson, H. R., Pierpont, M. E. and Gelb, B. D. (2000). Mutations in TFAP2B cause Char syndrome, a familial form of patent ductus arteriosus. *Nat. Genet.* **25**, 42-46.

Schilling, T. F., Piotrowski, T., Grandel, H., Brand, M., Heisenberg, C.-P., Jiang, Y. J., Beuchle, D., Hammerschmidt, M., Kane, D. A., Mullins, M. et al. (1996). Jaw and branchial arch mutants in zebrafish **1**, branchial arches. *Development* **123**, 329-344.

Schilling, T. F., Prince, V. and Ingham, P. W. (2001). Plasticity in zebrafish hox expression in the hindbrain and cranial neural crest. *Dev. Biol.* **231**, 201-216.

Schorle, H., Meier, P., Buchert, M., Jaenisch, R. and Mitchell, P. J. (1996). Transcription factor AP-2 essential for cranial closure and craniofacial development. *Nature* **381**, 235-238.

Stachel, S. E., Grunwald, D. J. and Myers, P. Z. (1993). Lithium perturbation and goosecoid expression identify a dorsal specification pathway in the pregastrula zebrafish. *Development* **117**, 1261-1274.

Thisse, C., Thisse, B., Schilling, T. F. and Postlethwait, J. H. (1993). Structure of the zebrafish snail1 gene and its expression in wild-type, spadetail and no-tail mutant embryos. *Development* **119**, 1203-1215.

Trainor, P. A. and Krumlauf, R. (2000). Plasticity in mouse neural crest cells reveals a new patterning role for cranial mesoderm. *Nat. Cell Biol.* **2**, 96-102.

Trainor, P. A., Melton, K. R. and Manzanares, M. (2003). Origins and plasticity of neural crest cells and their roles in jaw and craniofacial evolution. *Intl. J. Dev. Biol.* **47**, 541-553.

Trokovic, N., Trokovic, R., Mai, P. and Partanen, J. (2003). Fgfr1 regulates patterning of the pharyngeal region. *Genes Dev.* **17**, 141-153.

Trumpp, A., Depew, M. J., Rubenstein, J. L., Bishop, J. M. and Martin, G. R. (1999). Cre-mediated inactivation demonstrates that FGF8 is required for cell survival and patterning of the first branchial arch. *Genes Dev.* **13**, 3136-3148.

Tsang, M., Friesel, R., Kudoh, T. and Dawid, I. B. (2002). Identification of Sef, a novel modulator of FGF signaling. *Nat. Cell Biol.* **4**, 165-169.

Tucker, A. S., Yamada, G., Grigoriou, M., Pachnis, V. and Sharpe, P. T. (1999). Fgf-8 determines rostral-caudal polarity of the first branchial arch. *Development* **126**, 51-61.

Veitch, E., Begbie, J., Schilling, T. F., Smith, M. M. and Graham, A. (1999). Pharyngeal arch patterning in the absence of neural crest. *Curr. Biol.* **9**, 1481-1484.

Wall, N. A. and Hogan, B. L. (1995). Expression of a bone morphogenetic protein-4 (BMP-4), bone morphogenetic protein-7 (BMP-7), fibroblast growth factor-8 (FGF-8) and sonic hedgehog (SHH) during branchial arch development in the chick. *Mech. Dev.* **53**, 383-392.

Walshe, J. and Mason, I. (2003). Fgf signaling is required for formation of cartilage in the head. *Dev. Biol.* **264**, 522-536.

Zhang, J. A., Hagopian-Donaldson, S., Serbedzija, G., Elsemore, J., Plehn-Dujowich, D., McMahon, A. P., Flavell, R. A. and Williams, T. (1996). Neural tube, skeletal and body wall defects in mice lacking transcription factor AP-2. *Nature* **381**, 238-241.